Seismic vulnerability of historic brick masonry buildings in Vienna

Karic, Amel; Atalić, Josip; Kolbitsch, Andreas

Bulletin of Earthquake Engineering (2022) 20:4117–4145
https://doi.org/10.1007/s10518-022-01367-2

ORIGINAL ARTICLE

Seismic vulnerability of historic brick masonry buildings in Vienna

Amel Karic[1] · **Josip Atalić**[2] · **Andreas Kolbitsch**[1]

Received: 17 October 2021 / Accepted: 16 February 2022 / Published online: 10 March 2022

Abstract
This paper presents a seismic vulnerability analysis of historic brick masonry buildings in Vienna, Austria from the period of the Austro-Hungarian monarchy (1840–1918). The vulnerability study is based on comprehensive data from the devastating earthquake damage to the masonry buildings in Zagreb, Croatia on March 22, 2020, which are from the Austro-Hungarian monarchy and comparable to Viennese buildings from that period, as well as on comprehensive numerical structural analyses calibrated on in situ test series. The statistical analysis of the earthquake damage to the Zagreb masonry stock and the comprehensive numerical simulations, allowed profound conclusions about the proportional damage distribution over individual structural areas of the masonry buildings, considering construction-specific characteristics such as the building height, the structural regularity/irregularity or the construction type under the ground level. This study enhances the still limited knowledge about the vulnerability of the historic brick masonry buildings from the period of the Austro-Hungarian monarchy and allows extensive conclusions about the seismic vulnerability of these buildings.

Keywords Earthquake · Masonry buildings · Seismic vulnerability · Numerical structural analyses

1 Introduction

The risk assessment of the seismic vulnerability of historic brick masonry buildings is a challenging topic in Vienna, Austria due to the construction- and material-specific characteristics as well as the absence of seismic events with building damage. In Vienna, the

✉ Amel Karic
amel.karic@tuwien.ac.at

Josip Atalić
josip.atalic@grad.unizg.hr

Andreas Kolbitsch
andreas.kolbitsch@tuwien.ac.at

[1] Faculty of Civil Engineering, Vienna University of Technology, Vienna, Austria

[2] Faculty of Civil Engineering, University of Zagreb, Zagreb, Croatia

occurrence of earthquakes with building damage is observed in a very irregular sequence. Due to the rarity of earthquakes, the historic brick-masonry building stock has not been subjected to any tests so far in the last decades to be able to draw any conclusions on the seismic vulnerability. However, historical earthquakes have shown that the seismic risk of Vienna cannot be ignored (Hammerl and Lenhardt 2013). To provide a qualitative and realistic assessment of the vulnerability of the Viennese historic brick masonry buildings under seismic events, a comprehensive data base of observed structural damage to the masonry stock is essential. A pure extrapolation of historical earthquake damage, such as the well-documented damage to the Viennese stock caused by the historical earthquake of "Ried am Riederberg" in 1590 (Gutdeutsch et al. 1987) is limited and can only be done with caution because of the historically strong earthquake events which took place far in the past, there is no clear transferability to the characteristic masonry stock from the period of the Austro-Hungarian monarchy (Hammerl and Lenhardt 2013). Earthquake damage data of lower earthquake intensities are available, yet do not clearly identify the bearing capacity reserves of the masonry stock from the period of the Austro-Hungarian monarchy under seismic events (Duma 1988). For example, the last stronger earthquake in the Vienna area, the so-called "Seebenstein earthquake" in 1972, with an intensity of 6°–7° according to EMS-98 (Grunthal et al. 1998), resulted mainly in damage to non-structural elements of the historic brick masonry stock (Duma 1988). The observed damage, mainly at two- to four-story buildings, included hundreds of damaged chimneys, damage to parapets and balustrades, and a whole series of consequential damage from collapse in attics and on traffic areas. There were reports of slight damage in upper stories, such as plaster damage, small cracks in walls, and cracks in windowpanes. Building damage to structural components or partial building collapse were not reported in Vienna (Drimmel and Duma 1974).

This paper provides a comprehensive analysis not only of the global structural behavior, but also of the non-structural behavior under seismic influence of brick masonry buildings from the period of the Austro-Hungarian monarchy. With the main aim to gain more knowledge of the structural behavior of historic brick masonry under earthquakes and to analyze the still relatively limited knowledge about seismic vulnerability of the historic brick masonry stock in Vienna and to emphasize the influence of specific building characteristics on seismic safety. Earthquake damages of past seismic events, such as the Zagreb earthquake 2020 (Atalic et al. 2021b) or even the L'Aquila earthquake 2009 (Augenti and Parisi 2010), show that significant economic and ecological losses are due to damage to non-structural components. The potential for substantial damage from non-structural components, as well as local failure and local damage mechanisms in areas of lower seismicity are a further motivation for this detailed investigation. National as well as international building standards, such as according to Eurocode 8 (ÖN EN 1998-3 2013), FEMA P-154 (FEMA P-154 2015), SIA 269/8 (SIA 269/8 2017) or assessments, such as according to (Meskouris et al. 2001; D'Ayala and Speranza 2002; Achs and Adam 2012b) provide a valuable basis for the evaluation of existing buildings due to earthquakes. A good overview of possible assessment methods is given in (Calvi et al. 2006). The building standards often deal with different building types, which means that the specific properties of the Viennese historic brick masonry buildings cannot always be clearly covered.

In the last decades, intensive experimental and theoretical investigations have been carried out, which have contributed to a significant improvement of the knowledge about the dynamic structural behavior of historic brick masonry buildings in Vienna. Particularly experimental tests on constituents of the historic masonry (Furtmüller et al 2012; Dunjic 2018) up to tests on wall level (Zimmermann and Strauss 2012) were performed and efficient numerical material models (Lu and Heuer 2007; Furtmüller and Adam 2011)

were presented. Furthermore, in (Achs and Adam 2012a; Kopf and Adam 2014) extensive measurement investigations of the dynamic behavior provided valuable knowledge of the influence of individual structural elements (such as the partition walls, etc.) on the global dynamic system. The work of (Achs and Adam 2012b) presents a rapid-visual-screening (RVS) method for a rapid seismic assessment developed to historic brick masonry buildings, where both the physical vulnerability and the socio-economic vulnerability are considered and provides new findings of the vulnerability of historic brick masonry buildings. In addition, efficient numerical and analytical methods for describing the load-bearing behavior of individual historic masonry walls were presented in (Rudisch et al 2017; Moschen et al 2019).

The first part of this paper analyzes the seismic vulnerability of the historic brick masonry buildings based on the earthquake damage observed after the earthquake in Zagreb, Croatia on March 22, 2020. The considered buildings in Zagreb are from the period of the Austro-Hungarian monarchy from 1840 to 1918 and are comparable or identical to Viennese buildings from that period, as many structures were built by Austrian planners/builders. The analyze of the earthquake damage allow a qualitative and realistic assessment of the vulnerability of the historic brick masonry buildings. For a detailed damage analysis within the building typology, a building block in the Zagreb city center was used, which is representative for the historic brick masonry buildings of Zagreb. Based on the well-documented damage database (HCPI database 2020), extensive conclusions about the proportional damage distribution over individual structural areas of the masonry buildings are made possible. The statistical acquisition and processing of the damage data allowed the derivation of modified vulnerability functions (Schwarz et al. 2010) for individual structural areas, considering construction-specific characteristics such as building height, structural regularity/irregularity or construction type under the ground level (cellar, basement). Influences of weathering, past seismic events, war impacts or non-professional reconstructions/additions over the decades could not always be clearly determined. The criteria for determining the grade of damage (D0–D5) follow detailed rules, whereby the criteria are in accordance with the EMS-98 scale (Grunthal et al. 1998) as well as (Anagnostopoulos and Moretti 2008; Uros et al. 2020). The empirical vulnerability functions allow the comparison among individual structural areas as well as the evaluation of the proportional damage distribution under construction-specific characteristics. Through the statistical analysis the vulnerable structural as well as the non-structural areas can be located, and the underlying damage trends can be identified, which represents a significant increase in value, as the vulnerability of individual building areas of historic brick masonry buildings in Vienna is generally little known.

The second part of the paper presents an extended reliable evaluation of the structural behavior of the historic brick masonry buildings obtained by using probabilistic dynamic FE time history analysis (ANSYS). Considered are the cases (a) 5-story building and (b) 3-story building with regularity in plane and elevation that follow the concept from (Krakora and Bauer 2014). For a good comparison of the structural behavior under dynamic loading, the material behavior with its strong dissipative properties was calibrated using extensive in-situ shear test series on masonry walls of a 4-story masonry building (Dunjic 2018). To reproduce the full range of possible structural responses due to dynamic loading, accelerograms of past earthquakes with significant earthquake properties related to energy content, frequency content, amplitude and duration (Bommer and Acevedo 2004) were used and matched for the Vienna area. The earthquake engineering software Seismosoft (SeismoMatch 2020) allows to match of a site-specific target response spectrum by using real earthquake accelerograms. The use of test-based numerical simulations enabled a

significantly improved identification of critical structural areas in Viennese masonry buildings. Furthermore, the numerical simulations show excellent agreement with the critical structural regions presented in the first part of this work. Vulnerable structural areas under dynamic load were presented as the total strain ε_{tot} (Simo and Hughes 1998; Kita et al. 2020). The plastic strain allows to identify the areas in which local load shifting or material failure/crack formation take place (Dynardo 2018). The obtained results were given as maximum relative inter-story drifts (Meskouris et al. 2011) and peak horizontal floor acceleration amplification (PHFA/PGA) along the building height (Chaudhuri and Hutchinson 2004). For comparison, the currently valid thresholds according to EC 8 were also given and discussed.

2 Seismic vulnerability of historic brick masonry buildings – earthquake of Zagreb on March 22, 2020

The earthquake damage to the masonry buildings of Zagreb, Croatia, after the Zagreb earthquake on March 22, 2020, is used with the goal to identify and evaluate critical structural areas. The M_W5.4 earthquake of Zagreb was the strongest earthquake in Zagreb since the M_L6.2 earthquake of 1880 (Atalic et al. 2021b; Simovic 2000). The earthquake in 2020 showed a ground motion of more than 0.2 g and a maximum spectral acceleration of about 0.6 g at 0.1 s (Atalic et al. 2021b). The ground motion was felt throughout Croatia and even in parts of Austria (ZAMG 2020). In the area in and around Zagreb, seismic activity is significantly higher than in Vienna (ÖN B 1998-1 2017). The expected horizontal peak ground acceleration according to the Earthquake Hazard Map of Republic of Croatia for the Zagreb area is up to 0.28 g for a return period of a 475-year earthquake according to HRN EN 1998 (Herak et al. 2011) and up to 0.08 g for Vienna area (ÖN B 1998-1 2017). The Zagreb earthquake caused major damage to buildings, especially to the city's historical and cultural heritage, which showed significantly higher seismic vulnerability compared to buildings made of reinforced concrete or concrete frame buildings with unreinforced masonry infill walls. A pronounced damage pattern was found in the city center, especially in the three- to five-story masonry buildings from the period of the Austro-Hungarian monarchy to 1918 (Savor Novak et al. 2020; Atalic et al. 2021b).

2.1 Classification of buildings

For this study a perimeter building block with 35 historic brick masonry buildings in the Zagreb city center was selected. This block is representative of the Zagreb masonry buildings and serves as a basis for research investigations as well as possible retrofitting measures. In the investigated block area, masonry buildings with flexible ceiling and roof diaphragms predominate, which were built mainly before 1918. The buildings were classified based on extensive building data, construction plans and other recorded data. Based on the database (HCPI database 2020) and construction plans, it was possible to clearly identify the building construction (type of construction, year of construction, structural design, etc.), as well as to trace individual reconstructions/additions as far as possible. The characteristic masonry construction method consists of solid masonry bearing (longitudinal) walls in wall thicknesses of 30–90 cm and slender nonbearing (transverse) walls in wall thicknesses of 15–30 cm. The masonry structure was built of solid bricks laid in pattern and mainly lime mortar. Timber joist ceilings are the predominant type of ceiling. Massive

ceilings were used above the underground story (Savor Novak et al. 2020). The foundations were mostly made as masonry wall footing to distribute loads of the structural bearing walls to the ground. In most cases, the width of the wall foundation was usually the same width of the wall and was made by the same masonry material as the vertical structure wall. In some cases, underground walls were also reinforced. It should also be noted that due to the much stronger wall structures and with the massive ceiling structures, the underground stories have a much higher stiffness than the upper stories. The detailed construction plans allow a clear classification according to occurring building characteristics and provides the basis for an analysis for statistical comparison of emerging damage distributions under certain building characteristics. Furthermore, in the case of mixed construction types, e.g., different ceiling systems, the non-dominant type is neglected. Double classification occurs only when different systems occur with equal significance (D'Amato et al. 2020). Figure 1 shows the proportional distributions of the occurring building characteristics in the form of histograms as well as their cumulative percentage, which will be comprehensively investigated in the further study.

The distribution by building characteristics shows that about 80% of the buildings have a story number of 3 and 4 (without underground story and attic). The attics are primarily not extended. More than 90% of the buildings have an underground story (cellar, basements, or partial cellar/basements). A classification was also made according to the type of underground story. It was possible to identify 4 types of underground stories: buildings

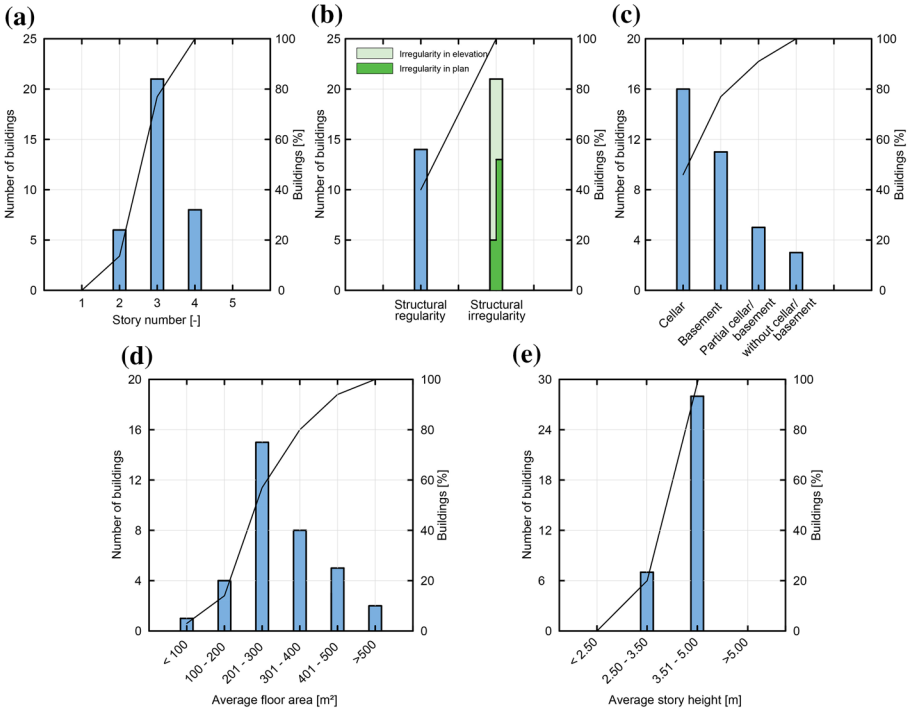

Fig. 1 Distribution of masonry building as function of **a** story number (without underground and attic story), **b** structural regularity/irregularity, **c** type of underground story, **d** average floor area and **e** average story height

with cellars, buildings with basements, buildings with partial cellars/basements and buildings without cellar/basement. Cellar means that it is completely below the level of the ground or curb. Basements (Souterrains) means that part of the room height of the basement is above the level of the ground or curb. The irregularity in plan is characterized by L-, T- or U-shaped plans where the floor area of the projecting building wing (A2) is greater than $0.15 \times A1$ (A1: floor area main building) or the ratio of building length to building width is > 4 (Achs and Adam 2012b). The classification as irregularity in elevation was made if several or all of the shear walls in individual stories (e.g. soft ground floor, etc.) were not present or were replaced by columns/piers (Achs and Adam 2012b). The distribution of average floor areas (Fig. 1d) and average story heights (Fig. 1e) is also shown. The individual building parameters are well dispersed among each other and are sufficiently available to provide a qualitative statement about the emerging damage trend under specific building characteristics. Influences of weathering, past seismic events, war impacts or non-professional reconstructions/additions over the decades could not always be clearly determined. Primarily, a poorer masonry quality is assumed, especially about mortar quality (Savor Novak et al. 2020). Based on the location of the building block (no slope) and the spatial distribution of the earthquake damage, which was not irregular, it can be assumed that the seismic events that occurred were very likely to be approximately the same over the building block area and that there were no significant influences from local ground amplification effects.

2.2 Definition of the grades of damage and damage patterns

To be able to evaluate individual structural areas, such as bearing and nonbearing masonry walls, staircase, ceilings and attic of the masonry buildings on the basis of damage indicators, the damage grades (D0–D5) are defined in accordance with the EMS-98 (Grunthal et al. 1998; Uros et al. 2020) as well as (Anagnostopoulos and Moretti 2008). These damage grades are given in detail in Fig. 2 with the corresponding example damage pictures as well as with the corresponding description. The building inspections and the detailed pictorial as well as written records of the earthquake damage (HCPI database 2020) immediately after the seismic events made it possible to classify the earthquake damage and to compare the damage distribution over individual structural areas. In this study, the criterion of maximum observed damage in the considered structural area is used to determine the grade of damage (D0–D5) (D'Amato et al. 2020). When defining the evaluation of the damage level, this study does not distinguish between structural areas, such as bearing and nonbearing masonry (e.g., partition walls, gable walls, etc.), in order to clearly identify the correlation between building characteristics and the damage distribution.

2.3 Statistical assessment of the seismic vulnerability

The observed earthquake damage is reproduced using modified empirical vulnerability functions (Schwarz et al. 2010). The proportional damage distribution over the individual structural areas of the analyzed building block with 35 historic brick masonry buildings is shown in Fig. 3.

It can be clearly seen that the most severe damage is recorded in the attic area. The damage percentage of very heavy damage (D4) in the attic exceeds 60% of the inspected buildings. The damages were the predominant throwing off of unbraced chimneys, partial

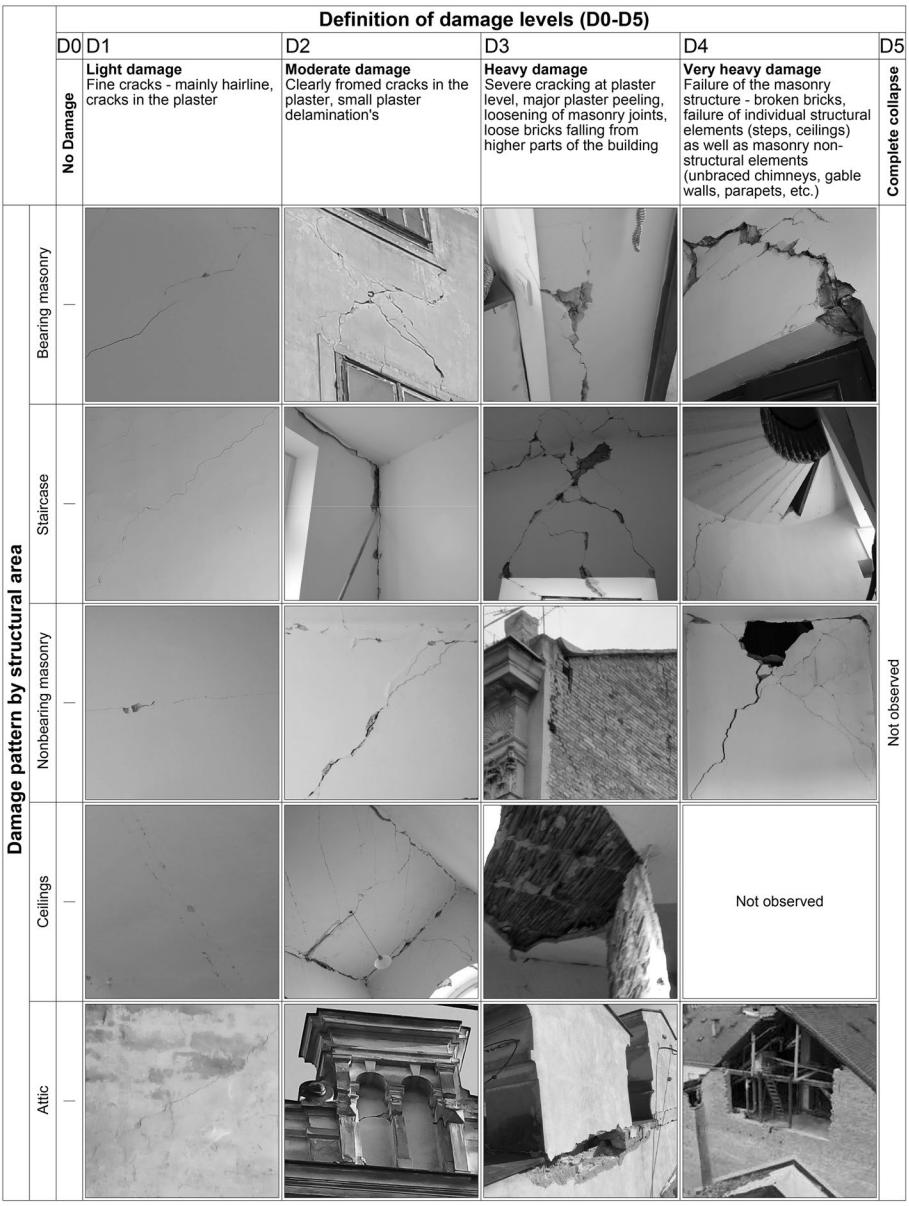

Fig. 2 Definition of damage grades and example patterns of damaged structural areas by the Zagreb earthquake on March 22, 2020. Author pictures: Mario Todoric (HCPI database 2020)

throwing off of brick gable walls and destroyed domes, parapets, roof structures and non-bearing masonry walls to the staircase (cf. Fig. 2).

The bearing masonry (primarily longitudinal walls) shows a moderate damage distribution with a proportional probability of occurrence of moderate damage (D2) of 29% and heavy damage (D3) of 31%. Very heavy damage D4 occurs to the bearing masonry in ≈

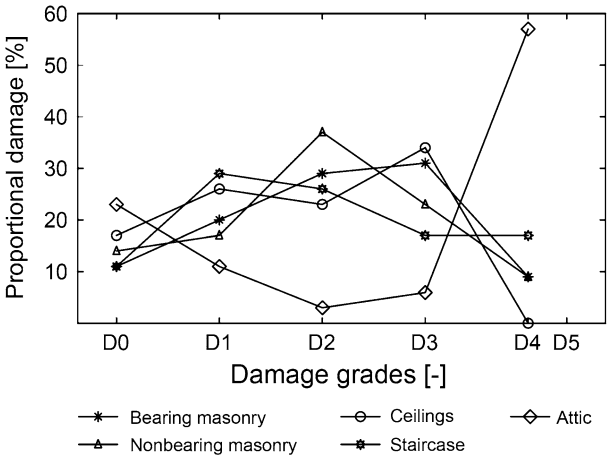

Fig. 3 Distribution of damage grades using empirical vulnerability functions (Schwarz et al. 2010) for the analyzed structural areas of the building block with 35 historic brick masonry buildings

10% of the structures inspected. The damage concentration was in areas of large stiffness changes and in areas of masonry openings (windows, doors). The nonbearing masonry shows a similar damage distribution. The damage concentration (shear and tensile cracks) was predominantly in areas of wall openings and in the connection areas to the bearing walls as well as to the ceilings and isolated shear cracks. Similarly, very heavy damage (D4) was recorded in some cases on the nonbearing walls between the attic and the staircase. Very heavy damage to the nonbearing fire walls was not recorded. Primarily, cracks in the nonbearing firewalls were observed in the connection areas (see Fig. 2) to the load-bearing longitudinal walls on the higher stories (Fig. 3).

The staircase represents the structural area of the masonry buildings that shows the highest percentage of damage (18%) of very heavy damage (D4) to structural building elements. Primarily, very heavy damage was identified in areas of window and door openings and in the connection areas of different wall stiffness—connection staircase/main building. In isolated cases, very heavy damage to staircase structures (destruction of individual steps, etc.) was also recorded.

The ceiling structures, mainly in the form of timber joist ceilings, did not show any structural damage. The damage patterns confirmed the typical flexible structural response that occurs under earthquake action, in where the damage, such as plaster cracking and spalling, was concentrated along the individual timber joists as well as the wall connection areas. The observed damage implies a significant bending stress on the individual timber beams as well as the relative deformations to the wall connection areas between the individual structural elements (Savor Novak et al. 2020).

In the underground stories, no predominant earthquake damage in the masonry and in the massive ceiling structures was found. A comprehensive reproduction of the Zagreb earthquake damage is shown in the works of (Savor Novak et al. 2020; Uros et al. 2020; Atalic et al. 2021b) as well as (Greguric, forthcoming).

2.4 Seismic damage distribution under certain building characteristics

The data collection confirmed that a higher damage density is not only to be expected due to the building type (vulnerability class B to EMS-98) or, for example, in areas of local soil amplification effects, but that building characteristics can also significantly

influence the damage distribution, primarily in the historic brick masonry buildings. Figure 4 illustrates the proportional damage distribution of the recorded maximum damage grades under specific building characteristics using empirical vulnerability

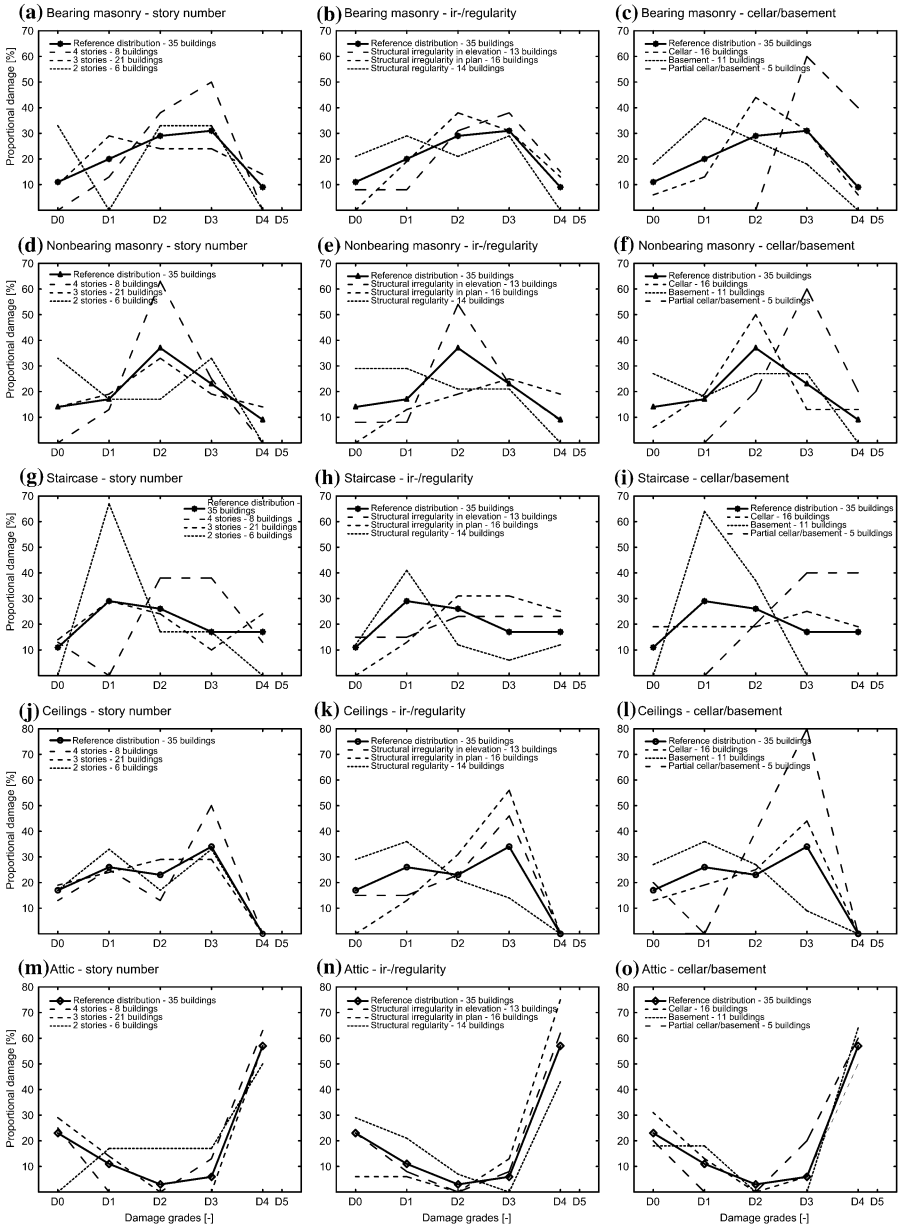

Fig. 4 Proportional damage distribution for individual structural areas (bearing and nonbearing masonry, staircase, ceilings and attic) considering specific building characteristics (story number, ir-/regularity and type of underground story) of the investigated building block

functions (Schwarz et al. 2010). It can be clearly seen that under certain building characteristics, previously described in Fig. 1, an emerging damage trend can be observed.

• **Building height**

The vulnerability functions in Fig. 4a, d, g, j, m illustrate the damage distribution in relation to the building height over the individual structural areas. It can be seen that as the number of stories increases, the number of undamaged structural areas such as bearing and nonbearing masonry, ceiling systems, decreases. Buildings with 4 floors show a clear increase in the proportional damage distribution of moderate (D2) and heavy damage (D3) in the bearing, nonbearing masonry (partition walls) and in the staircase, especially on higher building stories. In contrast to the shorter buildings (2 and 3 stories), earthquake damage is observed in all 4-story buildings. The observed damage trend among the building heights is also reflected in the ceiling areas, except that no very heavy damage (D4) is recorded due to the specific flexible construction type (timber joisted floors). A specific influence under building height on the distribution of damage in the attic could not be clearly identified. High seismic damage is noted in the attics across all building heights.

• **Structural regularity**

The resulting vulnerability functions as a function of regularity in plan and elevation (Fig. 4b, e, h, k, n) confirm their positive influence on the vulnerability of the masonry buildings due to earthquakes. A clear flattening of the higher degrees of damage over the individual structural areas can be observed. Very heavy damage is not detected in the bearing and nonbearing masonry. The average proportional damage percentage of undamaged structural areas is 24%. The positive influence is also observed in acceleration-sensitive elements in the attic with a lower proportional percentage (43%) of very heavy damage (D4). The vulnerability functions confirm that masonry buildings with regular arrangement of bearing structural elements achieve significantly lower vulnerability to seismic events compared to irregular arrangement.

• **Structural irregularity**

The comparison of the influence of the irregularity of load-bearing structural elements to the regularity shows a significant increase in the occurring damage grades of moderate (D2), heavy (D3) and very heavy damage (D4). The trend of damage increase occurs in all structural areas and confirms the negative influence on the dynamic structural response under earthquake. The highest proportional structural damage percentage of very heavy damage (D4) is recorded in the staircase of 25%, which is a result of the often-characteristic eccentric location of the staircase in the building floor plan and the often-poor connection to the main building. The proportional damage level of very heavy damage (D4) shows a significant increase in occurrence to over 75% in the attic (nonbearing structural elements).

• **Underground execution**

Remarkable is the trend of damage distribution that occurs under certain characteristics of the execution of the underground story (Fig. 4c, f, i, l, o). A partial cellar/basement leads to a significantly higher damage percentage of heavy (D3) and very heavy damage (D4) over all structural areas in the above-ground stories. Buildings with cellar (completely below the level of ground or curb) are characterized by a moderate damage distribution over the individual structural areas. The positive influence on the resulting damage distribution in buildings with a basement (Souterrain) is to be emphasized. Buildings with basements show a significant decrease in heavy (D3) as well as very heavy damage (D4) over

all structural areas. Due to the small number (3) of buildings without a cellar, it was not possible to produce a statistical comparison of the damage distribution.

In summary, it can be stated that the seismic vulnerability study of the historic brick masonry buildings of Zagreb confirms the higher degree of damage occurring under the known construction-specific building characteristics, such as increasing number of stories, irregularity in plan and elevation. The positive influence of regularity in plan and elevation on the resulting damage distribution was also illustrated (cf. Fig. 4). Also, certain types of cellar/basement designs, such as a partial cellar/basement, showed significant amplification effects in the damage distribution, which are rarely or not at all taken into account in the assessment in the current standards. It is illustrated that the large difference in the stiffness distribution of partial cellars/basements has a significant negative influence on the structural responses of the upper constructure under earthquake loads. In many studies concerning the assessment of earthquake damage or the construction of fragility curves, the assumption is made that a sufficiently rigid cellar/basement can be assumed, which does not seem to be appropriate, especially for masonry buildings with partial cellar/basements. Buildings with basements (Souterrains) in contrast to buildings with cellar, showed a flattening of heavy (D3) and very heavy damage grades (D4) in all structural areas. This is due to the lack of effect of stiffening with increasing embedment (Meinhardt 2008), as the masonry buildings, unlike new buildings, do not have a rigid foundation (concrete slab), as well as due to the characteristic construction (often without transverse walls and wall foundation), the vulnerability to seismic events is increased with increasing embedment. Work such as (Loli et al. 2015) has shown the influence of different foundation types in masonry buildings against dynamic effects. The influence of the brick-built walls and foundation of the historic masonry buildings and the associated soil-structure interaction on the structural response requires more detailed analysis. A possible positive effect on the structural response under seismic events, which could be achieved by a retrofitted foundation reinforcement (insertion of concrete slab), would be of essential importance in the historic brick masonry buildings, primarily in heritage buildings from that period. The vulnerability functions confirm that the influence of regularity/irregularity has a significant impact on the damage patterns across attics. Buildings with irregularities in the floor plan show significant amplification effects of the damage level in the attics, which are not observed in this way under other building characteristics. For example, no divergent damage trends could be identified in the attic under the building height, which would suggest similar acceleration responses in the attic under different building heights (2, 3 and 4 stories). It must also be noted that the block development of the buildings (building next to building) could have an influence on the individual structural responses, especially in the case of neighboring houses with different building heights, which could not be clearly reproduced in this work. It could only be observed that the occurring earthquake damage was more frequent for freestanding gable walls, especially for buildings that have a higher building height than the neighboring building.

The study confirms that specific building characteristics within the typological classification of the historic brick masonry building have a clear influence on the expected damage level as well as distribution over the individual structural areas. In the work of (Achs and Adam 2012b) an efficient rapid-visual-screening (RVS)-method for seismic assessment of historic brick masonry buildings with 9 structural parameters (SP) and 5 damage relevance parameters (DR) is presented. The influence of the presented structural parameters (ir-/regularity in plan, elevation, etc.) could be confirmed by the evaluation of the earthquake damage. In addition, other significant structure-specific parameters, such as the execution of the underground story or the high vulnerability of free-standing gable walls, etc., could

be identified as further influencing factors in the assessment method. A detailed overview of the RVS method for historic brick masonry buildings is given in (Achs 2011; Achs and Adam 2012b). In addition, a simple typological consideration of the earthquake damage due to the characteristic construction without reference to the presented constructional specificities easily leads to an overestimation of the earthquake intensity, primarily in areas of moderate seismicity, such as Vienna area (Drimmel and Duma 1974).

3 Nonlinear dynamic analysis of the behavior of the historic brick masonry buildings

Due to the rarity of earthquakes with building damage on the Viennese historic brick masonry stock, representative data on the seismic vulnerability are not available. Therefore, the vulnerability study on the comparable/ident masonry stock of Zagreb allowed a realistic and differentiated assessment of the complex structural response of this building typology under a strong earthquake event. The vulnerability assessment, however, contains qualitative results about the influence of certain specific building characteristics on the damage distribution, which is an essential basis for the assessment of the historic brick masonry buildings under seismic events. The second part of this work allows a comprehensive identification of possible structural responses of these Viennese buildings under dynamic loading, as well as the validation of critical structural areas in the masonry from the vulnerability study in the first part. The evaluation of the behavior of the historic brick masonry buildings under dynamic loading is achieved by reliable probabilistic numerical FE time history analysis (ANSYS). The cases (a) 5-story masonry building and (b) 3-story masonry building with a "typical" Viennese masonry building floor plan, which follows the concept from (Krakora and Bauer 2014), are used for the in-depth numerical analysis and are shown in Fig. 5. As described in the first part of the paper, the floor slabs in historic brick masonry buildings consist mainly of timber joist ceilings (Kolbitsch 1989). Only a low shear effect can be attributed to the timber joist ceiling systems due to their characteristic construction structure. The flexible structural response of the timber joist systems was confirmed in the first part of this paper. Likewise, crack opening widths of up to 5 cm to the load-bearing longitudinal walls could be observed in the investigation of the earthquake damage in Zagreb, which indicates the partially insufficient connections of the joist (timber joist—masonry). The area loads for the floor ceilings were considered to be 2.30 kN/m^2 (timber joist ceiling + upper construction) and the area load of the ceiling to the attic to be 3.50 kN/m^2 (timber floor ceiling + upper construction) and the roof construction to be 0.70 kN/m^2 according to (Krakora and Bauer 2014). The area loads of the unidirectional ceiling structures as well as the quasi-permanent values of the live loads (2.00 kN/m^2 in the floors and 1.00 kN/m^2 in the attic) were assigned to the load-bearing longitudinal walls (middle wall, outside walls) for each floor (see Fig. 5). Due to the design-related vertical ceiling load transfer, because of the larger area and the resulting of influence the middle wall is subjected to higher vertical loads than the longitudinal outside walls. For the determination of the masonry mass, the walls own weight is taken into account via the spatial models. Furthermore, as a consequence of the low influence of the roof structure on the global dynamic behavior, a modeling of the roof structure in the spatial model was not required. The expected low influence could be shown in the work (Achs 2011; Achs et al. 2011) by comprehensive measurement experiments in historic brick masonry stock in Vienna. As a result of the presence of timber joist ceiling systems with low shear strength and insufficient ceiling-wall connections the

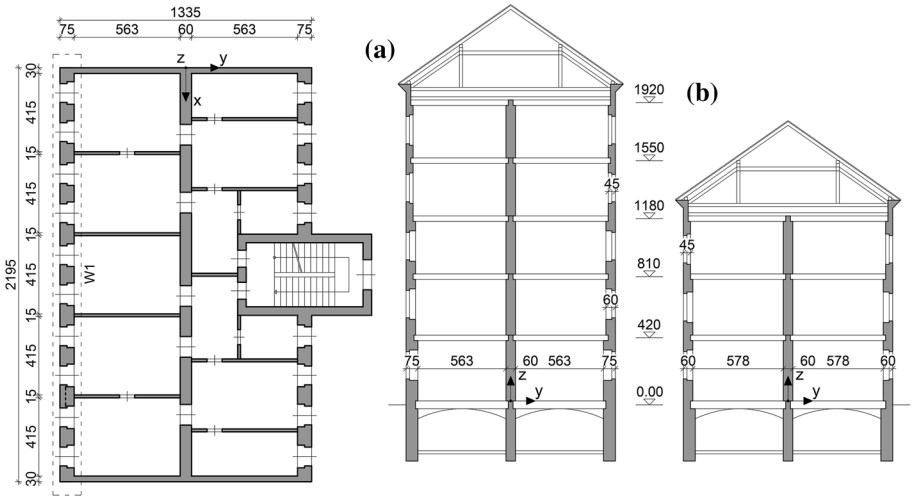

Fig. 5 Floor plan and elevation of the case studies (**a**) and (**b**) of a Viennese historic brick masonry reference building (dimensions in cm), modified from (Krakora and Bauer 2014)

individual masonry walls of the historic brick masonry buildings can be considered without the ceiling-masonry interaction. The possible higher global building strength due to the at least partial interaction between these elements is therefore not considered. This approach has also been followed in previous research, as (Rudisch et al. 2017; Moschen et al. 2019, etc.). For the scope of the study, the identification and location of critical structural areas in the masonry, the selected models are considered appropriate and allow also direct comparison with past research (Rudisch et al. 2017; Moschen et al. 2019, etc.). Moreover a good correlation of the observed critical structural areas from the first part of the paper is achieved in the numerical simulations (cf. Figs. 2, 6, 7 8, and 9).

3.1 Behavior of masonry under dynamic loading

The material- and construction-specific properties of the masonry require a complex system approach. The masonry structure with its specific material behavior is characterized by its strongly nonlinear material behavior, its material-specific failure mechanisms as well as its load redistribution (Schlegel et al., 2004). A hysteretic material behavior which can reproduce these material specific properties under dynamic loading is of essential importance (Bommer et al. 2004).

To describe the orthotropic masonry properties, a powerful macro model of the material database multiPlas is used for a robust numerical analysis and implemented in ANSYS. The material model based on the Ganz yield criterion (Ganz 1985) was extended to a spatial model and implemented in multiPlas (Dynardo 2018). The multi-surface yield condition (Fig. 6) is composed of individual failure criteria (yield criteria), which represent the individual failure mechanisms (stone, joint, bond failure, etc.) of a regular masonry bond (Dynardo 2018). The meaning of the individual yield criteria is also given in Fig. 6. The nonlinear stress–strain behavior of masonry is described by appropriate softening and hardening models (Schlegel 2004). In particular, by including the anisotropic deformation and cracking behavior that depends on the loading condition, as well as the inclusion of

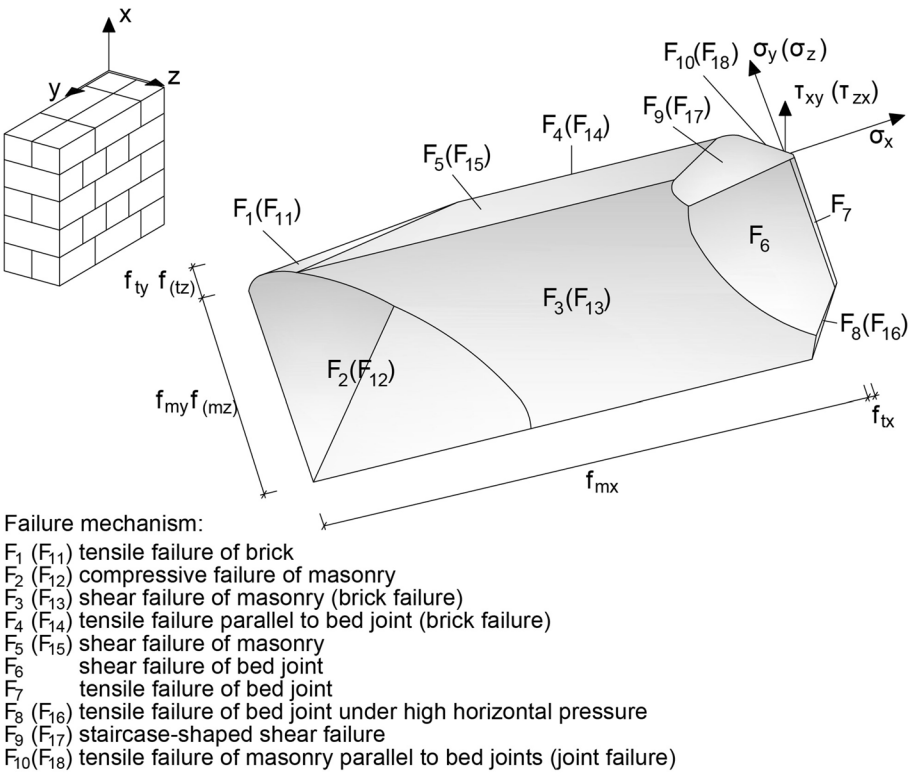

Fig. 6 Yield surface of the material model for regular masonry (Dynardo 2018; Schlegel 2004)

the masonry bond (brick dimensions), an efficient and realistic prediction capability of the masonry structure under cyclic loading is achieved.

The dynamic structural response of an old masonry building is strongly influenced by the degradation and hardening behavior. The implementation of such degradations enables the consideration of hysteretic material behavior under cyclic loading. The material damage is described by a decrease in initial strengths after failure. Exceeding the shear strength results in an exponential decrease of the cohesion c and a linear reduction of the initial friction angle to a residual friction angle. Accordingly, the transmission of shear forces via friction is only permitted to a limited extent. The tensile strength decreases progressively to zero due to progressive crack formation in the bearing joint. The dispersion of the crack widths is described by the fracture energy, while the softening is described by the plastic strain that occurs. For example, the occurrence of a tensile crack in the bearing joint causes the decrease in tensile strength and the decrease in cohesion due to the deterioration of the adhesion bond. The failure/opening of the mortar joint normal to the joint plane can be described in shear failure with the dilatancy angle (Dynardo 2018). A detailed description of the macro model can be found in the work of (Schlegel 2004).

At this point, it is also important to consider that other robust spatial material models for masonry have been presented in the literature, such as (Lu and Heuer 2007; Jordan 2011; Furtmüller et al. 2012), etc. The material models of (Lu and Heuer 2007) and (Furtmüller et al. 2012) are efficient simplifications of the failure functions defined by Ganz (Ganz

1985). Most importantly, the work (Furtmüller et al. 2012) presents a macromodel for historic masonry that was developed for historic brick masonry to achieve efficient structural analyses of walls in historic buildings. The performed comparative numerical simulations of experimental tests show impressively that the derived material models reproduce well the masonry failure under combined loading in the simulations.

3.2 Calibration of the masonry material model

The calibration of the masonry material model was achieved by well-documented in-situ shear tests on representative masonry walls as well as by three-brick test (Dunjic 2018). The verification on quasi-static test series in an existing Viennese historic brick masonry building allows a significantly improved description of the material behavior under combined loading. The test series could be successfully realized on four 30 cm thick partition walls of a 4-story building. The results of the in-situ shear tests are shown in Table 1 (column: In-situ shear tests, bold values). The initial shear strength at the plane of the bedding joint between the historic brick and mortar was determined on three-block tests (Dunjic 2018). Table 1 shows the in-plane damage limit states obtained from the in-situ shear tests (Dunjic 2018) according to (Tomazevic 1999). A comprehensive reproduction of the experimental procedure can be found in (Dunjic 2018). The mechanical properties of the late historic brick masonry of Vienna correlate with the mechanical masonry properties from Zagreb and confirm the strong similarity of the buildings. For example, masonry brick tests in 14 buildings from the Zagreb masonry stock resulted in compressive strength values of 6.45—24.20 MPa (Atalic et al. 2021a). The compressive strength of the Viennese bricks is 6.00—25.00 MPa for ordinary to good bricks (Kolbitsch 1989). This good correlation of mechanical properties is also observed for the other mechanical properties of the masonry walls. For comparison, other experimentally obtained damage thresholds from laboratory or in-situ experimental tests on whole houses or masonry walls are given from (D'Ayala 2013). The thresholds from (Zimmermann and Strauss 2012) refer to cyclic as well as quasi-static tests on Viennese historic brick masonry walls. Furthermore, the damage threshold values according to EC 8 (ÖN EN 1998–3 2013) are also shown.

Table 2 shows the material parameters achieved by the in-situ tests. The detailed material calibration is given in (Rudisch et al.2017) and (Karic et al. 2019). In addition, characteristic parameters from the literature (Furtmüller and Adam 2011; Furtmüller et al. 2012; Zimmermann and Strauss 2012) and (Schubert 2010) were used to optimize the material model. The brick geometry of the old Austrian format of $290 \times 140 \times 65$ mm (Kolbitsch 1989) with a head and longitudinal joints overlap was considered in the macromodel (Dynardo 2018). With the consideration of the strong degrading material properties (cf. Table 2) of the material model, a realistic analysis under dynamic loading is achieved. An adequate hysteretic material behavior was achieved and can be found in detail in the work of (Rudisch et al. 2017).

The dynamic characteristics of the generated spatial models' case (a) with $f_1 = 2.54$ Hz, $f_2 = 2.64$ Hz and case (b) with $f_1 = 3.38$ Hz, $f_2 = 4.38$ Hz correlate with dynamic experimental tests in similar masonry building in previous research (Achs et al. 2011). To generate acceptable dynamic structural responses, the structural damping is essential (Chopra 2019). Lehr's damping ratio of $\zeta = 4\%$ was estimated for both structural models (Achs 2011), which would appear appropriate for direct comparison of the structural responses (Cruz and Miranda 2016). Structural damping is accounted by the classical Rayleigh damping

Table 1 Performance drift value for damage limit states

Limit state	In-situ shear tests (Dunjic 2018)		(Zimmermann and Strauss 2012)		(D'Ayala 2013)		EC 8 Part 3 (ÖN EN 1998–3 2013)	
	In-plane		In-plane		In-plane	Out-of-plane	In-plane	Out-of-plane
	Drift range [%]	ϕ [%]	Drift range [%]	ϕ [%]	Drift range [%]			
Damage limitation (DL)/cracking limit	**0.16–0.31**	**0.22**	0.17–0.81	0.36	0.18–0.23	0.33		
Significant damage (SD)/maximum capacity	**0.92–1.94**	**1.24**	0.47–2.29	1.02	0.65–0.90	0.88	0.4–0.6	0.8–1.2 (H_0/D)
Near collapse (NC)	**1.02–2.02**	**1.72**	0.64–2.80	1.47	1.23–1.92	2.30	0.53–0.8	1.07–1.6 (H_0/D)

Table 2 Material parameters of the calibrated macro model (Karic et al. 2019)

Parameters	Physical unit
Elastic properties	
E-modulus of masonry normal to bed joints (x-direction)	$E_x = 850$ [N/mm^2]
E-modulus of masonry normal to head joints (y-direction)	$E_y = 283$ [N/mm^2]
E-modulus of masonry normal to longitudinal joints (z-direction)	$E_z = 283$ [N/mm^2]
Poisson's ratio	$v_{xy} = v_{yz} = v_{xz} = 0.026$ [–]
Shear modulus—xy	$G_{xy} = 102$ [N/mm^2]
Shear modulus—yz, xz	$G_{yz} = G_{xz} = 76.5$ [N/mm^2]
Strength parameters	
Uniaxial compressive strength of masonry normal to bed joints	$f_{mx} = 3.69$ [N/mm^2]
Uniaxial compressive strength of masonry normal to head joints	$f_{my} = 2.46$ [N/mm^2]
Uniaxial compressive strength of masonry normal to longitudinal joints	$f_{mz} = f_{my} = 2.46$ [N/mm^2]
Uniaxial tensile strength of masonry normal to bed joints	$f_{tx} = 0.01$ [N/mm^2]
Uniaxial tensile strength of masonry normal to head joints	$f_{ty} = 0.14$ [N/mm^2]
Uniaxial tensile strength of masonry normal to longitudinal joints	$f_{tz} = f_{ty} = 0.14$ [N/mm^2]
Residual tensile strength	$f_{tr} \sim 0$ [N/mm^2]
Cohesion of bed joints	$c = 0.026$ [N/mm^2]
Residual cohesion of bed joints	$c_r \sim 0$ [N/mm^2]
Friction angle of bed joints	$\varphi = 38$ [°]
Residual friction angle of bed joints	$\varphi_r = 22$ [°]
Dilatancy angle of bed joints	$\psi = 30$ [°]
Mode I fracture energy—tensile failure normal to bed joints	$G_{FF1} = 0.004$ [Nmm/mm^2]
Mode I fracture energy—tensile failure of stone (horizontal)	$G_{FS1} = 0.015$ [Nmm/mm^2]
Mode II fracture energy—shear failure of bed joints	$G_{FF2} = 0.080$ [Nmm/mm^2]
Softening variable (plastic strain)	$\kappa = 2 \times 10^{-3}$

(Rayleigh and Lindsay 1945) with coefficients $\alpha = 0.656$ (case (a)) and 0.959 (case (b)) and $\beta = 0.00244$ (case (a)) and 0.00164 (case (b)) (Cruz and Miranda 2017; Song and Su 2017).

3.3 Seismic input for analysis—Earthquake scenarios for the Vienna area

To evaluate the seismic vulnerability of historic brick masonry buildings, ground accelerograms are considered that would correspond to specific earthquake scenarios in the Vienna area. The selection of appropriate seismic ground motion recordings is the prerequisite to identify the full range of possible structural responses under dynamic loading with appropriate earthquake properties based on energy, frequency content, amplitude and duration (Iervolino and Cornell 2005). In this study selected earthquake scenarios (action groups) are considered, where each action group is defined by specific target response spectra. To provide a robust seismic vulnerability analysis, 5 possible earthquake scenarios for the Vienna area are considered. The single earthquake scenarios represent seismic events for the Vienna area with the exceedance probabilities of 95% (very frequent earthquakes), 50% (frequent earthquakes), 20% (occasional earthquakes), 10% (rare earthquakes) and 2% (very rare earthquakes) in 50 years (ÖN

B 1998–1 2017). These earthquake scenarios include a total of 30 (6 each) different spectrum compatible acceleration records. The reference ground acceleration (a_{gR}) for Vienna south of the Danube is 0.80 m/s^2 (ÖN B 1998–1 2017). Furthermore, the elastic response spectrum type 1 with 5% damping according to Eurocode 8 (ÖN B 1998–1 2017), Importance Class II and Soil Class A were selected. The corresponding elastic target response spectra S_a for the considered groups of actions are shown in red color, the response spectra of the individual records (gray lines) and the median of these spectra (black line) are shown in Fig. 7. The spectrum matching was achieved by the earthquake engineering software SeismoMatch (SeismoMatch 2020). The spectral matching methods are based on (Hancock et al. 2006; Atik and Abrahamson 2010) and allows to match of a site-specific target response spectrum by using real earthquake data.

The comparison of the median spectra with the target spectra of each action group shows good agreement in the range of the base period of the brick masonry buildings, which are between 0.25 s and 3.00 s (Moschen et al. 2019). In Table 3 the previously presented action groups are recorded. Furthermore, the maximum standard deviation of the logarithmized earthquake spectra ($\sigma_{Ln(Sa),max}$) is also reproduced as a measure of dispersion, which is comparable to results from previous research (Moschen et al. 2019).

In the work (Moschen et al. 2019), earthquake sets "Viennese ground motion set" are presented for the Vienna site, which are compatible with the target spectrum of the

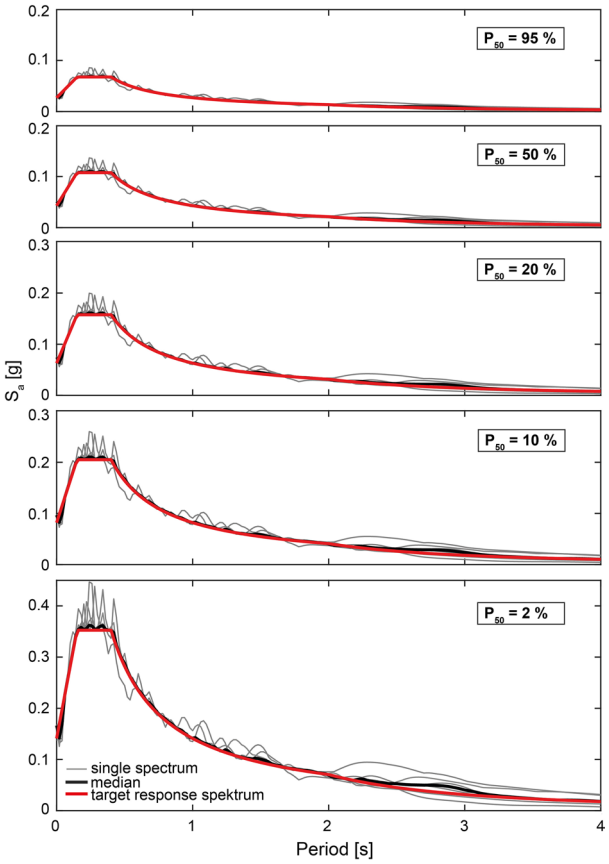

Fig. 7 Response spectra for the defined hazard levels. Response spectra of the individual records (gray), median spectra (black) and target spectra (red)

Table 3 Definition of the action groups/hazard levels

P_{50} [%]	T_L in years	a_g [m/s^2]	$a_{g,max}$ [m/s^2]	$\sigma_{Ln(Sa),max}$
95	16.7	0.26	0.31	0.5470
50	72	0.43	0.49	0.5466
20	225	0.62	0.73	0.5466
10	475	0.80	0.95	0.5462
2	2475	1.39	1.64	0.5464

Table 4 Parameters of the selected original ground motion (PEER 2010)

Event name	RSN	Station name	Year	M_W	Mechanism	PGA [g]
Friuli	125	Tolmezzo	1976	6.5	Reverse	0.35
Kobe	1107	Kakogawa	1995	6.9	Strike Slip	0.34
Landers	879	Lucerne	1992	7.3	Strike Slip	0.78
Loma Prieta	767	Gilroy Array	1989	6.9	Reverse Oblique	0.37
Northridge	963	Castaic, CA–Old Ridge Route	1994	6.7	Reverse	0.57
Trinidad	421	Rio Dell Overpass, E Ground	1983	5.7	Strike Slip	0.19

standard (EN 1998-1 2013) and provide another possibility for effective nonlinear time history calculations in the design load case. Furthermore, Table 4 summarizes the real earthquake data used to generate the defined response spectra.

The earthquake scenario "very frequent Earthquake" ($P_{50}=95\%$) represents the last strong earthquake, the so-called "Seebenstein earthquake" in 1972, in the Vienna area. A maximum ground acceleration of 0.027 g for the recorded ground motion (E-W) was documented at the Central Institute for Meteorology and Geodynamics (ZAMG) (Drimmel and Duma 1974). In the urban areas of increased damage intensity (predominantly no damage to structural masonry, cf. introduction), a twofold to threefold amplitude amplification due to unfavorable site factors with "resonance power" is assumed (Drimmel and Duma 1974).

3.4 Dynamic structural analysis results

The numerical simulations allow a comprehensive reproduction of the structural behavior considering the strongly degrading material properties under dynamic loading as well as the interaction of individual structural areas. To identify critical structural areas in the masonry structure, the results are presented as total strain ε_{tot} (Simo and Hughes 1998; Kita et al. 2020). The plastic strain is a scalar measure of the plastic strain tensor and shows the quantitative activity and can be used to identify the areas in which local load shifting or material failure / crack formation take place (Dynardo 2018). The results of the simulation and the observed damage trend in the structural masonry correlate with the damage patterns of the masonry stock in Zagreb. In this work, the seismic vulnerability is shown by the simulation results of the more vulnerable structural building direction, the transverse direction. Based on the limited state of knowledge the influence of the often-connected neighboring buildings was neglected in this work. For example, Fig. 8 illustrates the obtained simulation results of the considered cases (a) and (b) under the seismic event

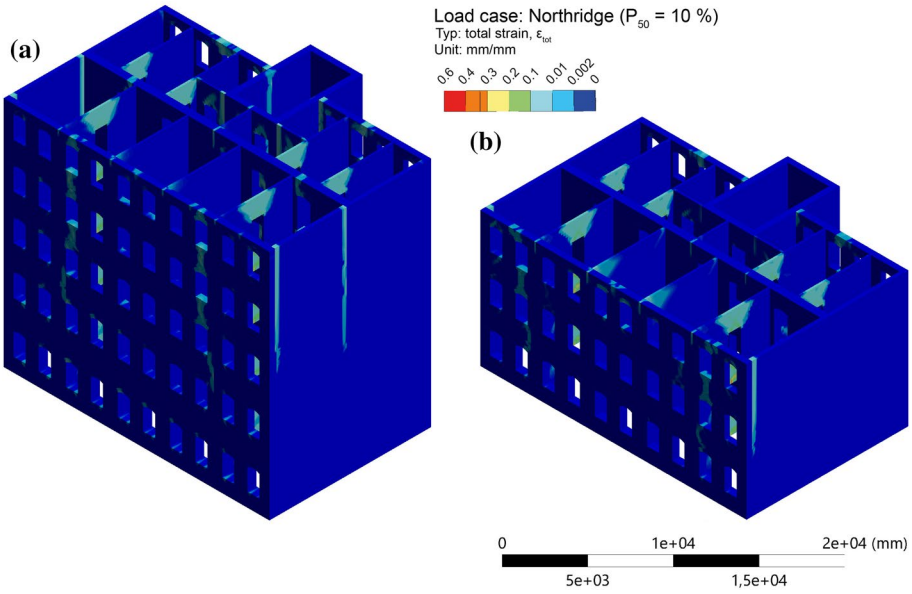

Fig. 8 Structural behavior of the masonry building under earthquake simulation (LC: Northridge $P_{50} = 10\%$) in transverse direction: **a** 5-story masonry building and **b** 3-story masonry building

$P_{50} = 10\%$. The generated structural responses confirm that with increasing stress, plastic deformations are concentrated in structural areas with large stiffness differences, such as in connection areas from nonbearing masonry walls to bearing masonry walls or from staircase walls to bearing/nonbearing masonry walls, as well as in structural areas of masonry openings (cf. Fig. 2). In above all, connection areas in nonbearing masonry walls represent a band of stronger stress, occasionally also characterized by shear cracks in the nonbearing masonry walls. The example damage pattern for nonbearing masonry with damage level D3 of the first part of the work (Fig. 2) also confirm the stress conditions occurring in the connection area firewall and bearing masonry (longitudinal wall) and confirm the good correlation of the plastic strain patterns (Fig. 8) obtained.

Exceeding the allowable material strength in the connection areas of the transverse walls can lead to failure of the connection areas of the transverse walls up to failure of the longitudinal walls (out-of-plane failure mechanism) and especially of the street-side masonry parapets. This out-of-plane failure mechanism was also observed in the buildings in the first part of the work, where the opening widths in the out-of-plane behavior of some longitudinal walls were up to 5 cm (HCPI database 2020). To achieve a better knowledge of the occurring critical structural areas, representative structural areas are subsequently selected and shown in Fig. 9. Figure 9 shows the typical plastic strain patterns under the seismic events, which were also observed in the partition's walls of the historic masonry buildings in Zagreb (see Fig. 2). For non-disturbed nonbearing masonry walls (without masonry openings), the plastic strain concentrations can be assigned to the wall connection areas as well as shear failure in higher lying areas. In case of disturbed nonbearing masonry walls (with masonry openings), the critical structural area is the masonry disturbances, which is characterized by the interaction of the individual masonry walls under dynamic influence with plasticization of the masonry beams and redistribution of tensile and shear stresses

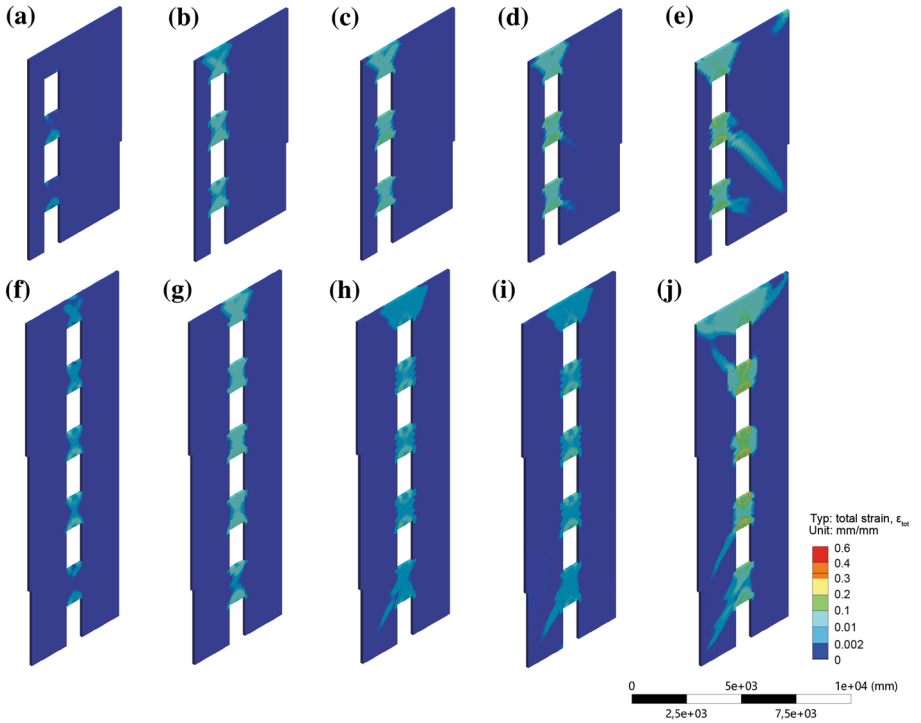

Fig. 9 Structural behavior of representative nonbearing masonry walls under specific earthquake scenarios: **a**–**e** courtyard-side partition of the case (**b**); **f**–**j** street-side partition of the case (**a**). Seismic groups: **a**, **f** $P_{50}=95\%$; **b**, **g** $P_{50}=50\%$; **c**, **h** $P_{50}=20\%$; **d**, **i** $P_{50}=10\%$; **e**, **j** $P_{50}=2\%$

that cannot be absorbed (Karic and Kolbitsch 2020). Both cases show typical plastic strain patterns (characteristic cross-shaped cracks as well as shear cracks) and are characterized by stronger plasticization. Under good replication of the hysteretic material behavior, a robust structural behavior is formed and a good agreement of the plastic strain concentrations with the observed earthquake damage on the old masonry stock of Zagreb is enabled.

The bearing capacity evaluation under the seismic events are reproduced using maximum relative inter-story drifts (ID) according to (Meskouris et al. 2011). Figure 10 shows the maximum relative inter-story drifts obtained from the numerical analyses, the mean value (m), and the standard deviation $m \pm \sigma$. For comparison, the normative maximum bearing capacity threshold of 0.4% (in-plane) according to EC 8 (ÖN EN 1998–3 2013) and the damage thresholds of 0.22% (damage limitation—DL), 1.24% (significant damage—SD) and 1.72% (near collapse—NC) obtained from the in-situ shear tests are also given (see Table 1). The earthquake scenarios "very frequent Earthquakes" and "frequent Earthquakes" confirm the recorded historical earthquake data of the Seebenstein earthquake (Drimmel and Duma 1974), where predominantly the elastic material behavior was activated and no damage to the structural masonry of the buildings was detected (Duma 1988). The earthquake scenario "Occasional earthquakes" lies within the range of initial crack formation in the structural masonry. The earthquake scenario "rare earthquake" represents the design earthquake for the Vienna area. The structural responses do not follow an easily detectable causality due to the strongly dissipative effects of masonry construction

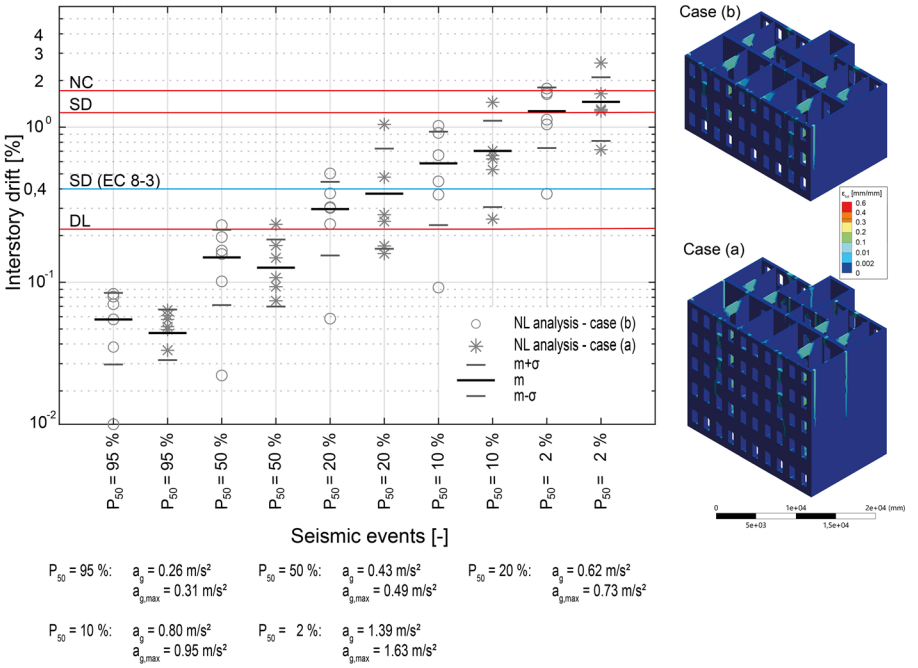

Fig. 10 Distribution of maximum relative inter-story drift [%] under seismic groups

under increasing strong earthquake phases. Case (a) is characterized by more increasing plastic activity. Both structural models respond in the nonlinear range, whereby on average the maximum load capacity was not reached. The "Very Rare Earthquake" would push the masonry stock to its horizontal structural limits (near collapse), both in- and out-of-plane structural behavior. Compared to the experimentally determined damage thresholds (DL, SD, NC), the Eurocode 8 (ÖN EN 1998–3 2013) is on the conservative side and would consider the old stock under the design earthquake case (rare earthquake) near collapse.

3.5 Dynamic non-structural analyses results

Non-structural masonry (gable walls, parapets, chimneys, etc.) represents the most vulnerable area for high damage under moderate seismicity based on their specific design (often slender masonry structures without significant anchorage) (Kolbitsch 2012), which has been clearly shown by the earthquake damage of past earthquakes in Vienna (Drimmel and Duma 1974), (Gutdeutsch et al. 1987) as well as by the earthquake damage in Zagreb 2020 (Atalic et al. 2021b) and 1880 (Simovic 2000). Non-structural masonry represent acceleration and/or displacement sensitive elements (Meskouris et al. 2011). For representative damage identification or for pre-quantification of potential local damage to and through acceleration-sensitive masonry elements, the simulation results are summarized in terms of absolute horizontal floor acceleration amplifications ($\Omega = \text{PHFA/PGA}$), the mean (m) and the standard deviation $m \pm \sigma$ over the normalized building height. The simplified standard design approach according to Eurocode 8 is also given for comparison. The acceleration responses show a significant scatter across individual masonry walls. The wall 1 (cf.

Fig. 5) was identified as the most acceleration-sensitive element in both cases. The acceleration responses of the individual wall elements (fire wall, partition wall, etc.) turn out differently, as also shown in (Rudisch et al. 2017). The diagrams in Fig. 11 illustrate the absolute horizontal floor acceleration amplifications Ω of wall 1 (cf. Fig. 5) over the height for the case (a) and case (b). The acceleration responses in plane (firewall, partition, etc.) are lower than the acceleration responses for walls out of the plane (longitudinal walls). A detailed reproduction of the acceleration responses in plane of individual load-bearing elements of historic brick masonry buildings is given in the works of (Rudisch et al. 2017, Karic et al. 2019 and Moschen et al. 2019) and are comparable to this work. The results in Fig. 11 show that the absolute horizontal floor acceleration distributions over the building heights among the individual seismic events have significant amplification and scattering in the structural responses. The cases (a) and (b) generate a different acceleration response over the building height. It can be observed that for weaker earthquakes ($P_{50}=95\%$ to $P_{50}=20\%$) the acceleration responses are significantly higher, primarily in case (b). Under increasing earthquake phases, a significant decrease in acceleration amplification is generated, that is mainly due to the pronounced nonlinearity caused by the cracking of the masonry structure and the resulting stiffness reduction (Bommer et al. 2004). The acceleration amplification in case (b) and case (a) during the very rare earthquake ($P_{50}=2\%$) is similar acceleration amplifications with $\Omega \approx 4$ and confirms the vulnerability function of according to the building height (Fig. 2-m: Attic—story number), which did not allow to identify any different trends of earthquake damage in Zagreb according to the building height in the attic. The results also confirm the vulnerability of earthquake-induced damage to non-structural components in the attic of shorter masonry buildings. It can be also observed that the simplified linear design approach according to EC 8, especially for the case (b), underestimates the resulting structural responses of acceleration-sensitive structural elements.

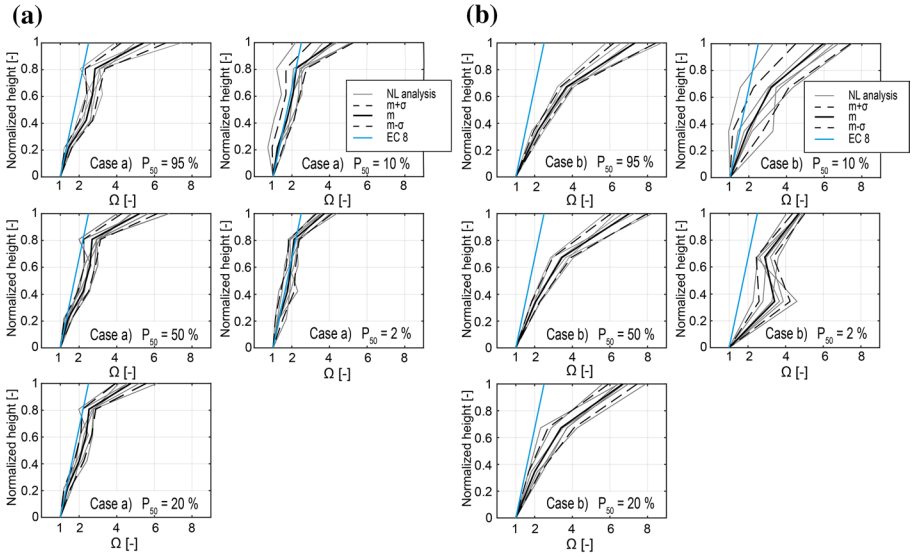

Fig. 11 Distribution of the absolute horizontal floor acceleration amplification Ω (PHFA/PGA) for W1 for the case (**a**) and (**b**)

It should also be emphasized that earthquake scenarios with very frequent and frequent occurrence can cause significant damage to non-structural building elements as a result of large dynamic amplification effects, as confirmed by the observed damage resulting from the Seebenstein earthquake 1972 (Duma 1988) with a maximum ground acceleration of 0.027 g for the recorded ground motion (E-W) at the Central Institute for Meteorology and Geodynamics (ZAMG) (Drimmel and Duma 1974). The Seebenstein earthquake damages resulted from the dropping of chimneys, parapets, balustrades of buildings. The strong acceleration responses of the street-side walls (W 1) also correlate with the 1972 earthquake damages, where severe damage as well as collapses of the stone ballustrades and roof cornices were observed (Drimmel and Duma 1974). Numerous chimneys dropped from shorter buildings, probably because of the strong acceleration amplification under the linear structural response. The numerical simulations confirm that the non-structural building elements, especially on the attic level, have high vulnerability due to the characteristic structural responses resulting from dynamic loading.

In conclusion, the numerical structural simulations under dynamic loading confirm the identified structural vulnerabilities of the historic brick masonry buildings and reliably reproduce the hysteretic material behavior under dynamic loading. It is also important to note that the cases considered (a) and (b) have a regular arrangement of load-bearing structural elements and that the identified building characteristics from the first part of the paper and their influence on the dynamic structural behavior should be considered in the building assessment against seismic events.

4 Conclusions

This paper contributes to the seismic risk analysis of the historic brick masonry buildings. Due to the relatively limited knowledge about the seismic vulnerability of the masonry stock in Vienna, a vulnerability assessment for a seismic risk analysis was achieved in two steps: The nonlinear numerical simulations and the statistical analysis of the earthquake damage at the historic brick masonry stock of Zagreb (Croatia) after the M_W5.4 earthquake event on March 22, 2020 (Atalic et al. 2021b). The numerical results are characterized by a good agreement with the critical brick masonry areas observed from the earthquake damage of Zagreb and past historical earthquakes in Vienna (Duma 1988).

The main results of the work are summarized below:

(1) The most vulnerable structural area of the masonry buildings (cf. Fig. 3) is the attic area, predominantly because of significant damage to the specific non-structural building elements (unbraced chimneys, parapets, gable walls, etc.). The specific strong acceleration amplification over the building height favors a high damage rate in the attic, also in shorter masonry buildings.
(2) The staircases are at higher risk primarily due to their specific, often very eccentric location in the building floor plan and the often-poor connection to the main building.
(3) The damage concentration in the structural and non-structural masonry is mainly found in areas of large stiffness change (connection areas, masonry openings, etc.), cf. Figure 8. Failure of the connection areas (structural/non-structural masonry) favor the out-of-plane failure mechanism and especially of the street-side parapets.

(4) The flexible load-bearing of the timber joist ceiling structures and partial insufficient connections to the masonry walls were confirmed, thereby increasing the potential for out-of-plane masonry failure.
(5) A positive influence on the damage distribution (less damage) in the structural masonry under earthquakes was demonstrated for shorter building heights, regular arrangement of structural elements and buildings with a basement (Souterrain).
(6) A clearly negative influence on the damage distribution in the structural masonry was observed for higher building heights, irregular arrangement of load-bearing building elements and partial execution of underground stories.
(7) The activation of the nonlinear material behavior under strong earthquake phases leads to similar acceleration responses in attic levels regardless of building height (cf. Fig. 4 m and Fig. 11). For less heavy earthquake events, the predominant linear structural response leads to much stronger acceleration responses in the attics, which increases the susceptibility to nonstructural damage even for more frequent weaker earthquake events, see Fig. 11.
(8) The simplified linear design approach according to Eurocode 8 is not suitable to reproduce the acceleration distribution over the building height, primarily of shorter masonry buildings.
(9) The common assumption that the underground story can be considered sufficiently rigid in the building assessment requires a more detailed analysis due to the construction-specific design, such as basement, cellar or a partial cellar/basement. The influence of the soil-structure interaction due to the missing concrete ground slab and the resulting lack of the positive effect of increasing embedment justifies a more detailed investigation.

The empirical vulnerability functions (cf. Fig. 4) of the first part of the work enabled the clear identification and correlation of emerging damage trends under construction-specific building characteristics. This paper underlines the fact that a purely typology-based building assessment without consideration of specific building characteristics does not always appear to be appropriate for qualitative earthquake mitigation. In addition, knowledge of susceptible structural areas as well as the influence of specific building features on seismic safety provides a comprehensive basis for anticipatory seismic retrofitting of the historic brick masonry buildings from the period of the Austro-Hungarian monarchy. For example, the retrofitting of a concrete ground slab and RC ceilings (e.g. the attic) with appropriate anchoring could lead to a significant stabilization of a solid historic brick masonry building. The positive effect of reinforced ceilings could be shown for example in (Celik and Sesigur 2010; Karic et al. 2019). A possible positive effect on the structural response under seismic events, which could be achieved by a retrofitted foundation reinforcement (insertion of ground slab), would be of essential importance in the historic brick masonry buildings, primarily in heritage buildings in Vienna. The stabilization of freestanding gable walls and freestanding parapets/balustrades and retrofitting/reinforcement of chimneys would reduce earthquake damages.

This paper identifies structural vulnerabilities as well as the influence of certain building characteristics on the damage distribution and thereby provides an important basis to evaluate existing building assessments for the historic brick masonry buildings in Vienna. Due to the strong degrading structural effects under dynamic loads, which are not expected for new buildings, the seismic evaluation of both structural and

non-structural could be improved based on the knowledge gained to reach an acceptable level of vulnerability as well as the retrofit level.

Acknowledgements We would like to thank Dynardo GmbH for providing a multiPlas-marketing license. Further gratitude is due to the numerous colleagues from the Faculty of Civil Engineering, University of Zagreb, Croatia, as well as to all the volunteers who carried out comprehensive building inspections and documentation after the earthquake.

Authors contribution All co-authors have contributed to the manuscript.

Funding Open access funding provided by TU Wien (TUW). No funding was received for conducting this study.

Declarations

Conflict of interest The authors declare that they have no conflict of interest.

Consent to participate All the authors agreed to participate in the writing of this manuscript.

Consent for publication All the authors agreed to submit this manuscript.

References

Achs G, Adam C, Benkö A, Brusatti W, Fritz M, Furtmüller T, Kopf F, Pietsch M, Schäfer D, Strauss A, et al (2011) Erdbeben im Wiener Becken - Beurteilung Gefährdung Standortrisiko [Vienna Basin Earthquake - Hazard Site Risk Assessment]. Grasl Druck & Neue Medien GmbH, Vienna, Austria (in German)

Achs G, Adam C (2012a) Assessment of the global dynamic behavior of a historic residential brick-masonry building in Vienna. In: Life-cycle and sustainability of civil infrastructure systems: proceedings of the 3rd international symposium on Life-Cycle Civil Engineering (IALCCE 2012). Vienna, Austria. CRC Press, London. https://doi.org/10.1201/b12995

Achs G, Adam C (2012) Rapid seismic evaluation of historic brick-masonry buildings in Vienna (Austria) based on visual screening. Bull Earthq Eng 10:1833–1856. https://doi.org/10.1007/s10518-012-9376-5

Achs G (2011) Erdbebengefährdung von Gründerzeithäusern: Beurteilung, Klassifizierung und experimentelle Untersuchungen [Seismic Hazard of Historic Residential Buildings: Evaluation, Classification and Experimental Investigations]. Dissertation, Vienna University of Technology (in German)

Anagnostopoulos S, Moretti M (2008) Post-earthquake emergency assessment of building damage, safety and usability - Part 1. Soil Dyn Earthq Eng 28:223–232. https://doi.org/10.1016/j.soildyn.2006.05.007

Atalic J, Todoric M, Uros M, Savor Novak M, Crnogorac M, Lakusic L (2021a) Potresno inzenjerstvo, obnova zidanih zgrada [Earthquake engineering, renovation of masonry buildings]. Faculty of Civil Engineering Zagreb, Zagreb, Croatia (in Croatian)

Atalic J, Urus M, Savor Novak M, Demsic M, Nastev M (2021b) The MW5.4 Zagreb (Croatia) earthquake of March 22, 2020: impacts and response. Bull Earthq Eng 19:3461–3489. https://doi.org/10.1007/s10518-021-01117-w

Atik LA, Abrahamson N (2010) An Improved Method for Nonstationary Spectral Matching. Earthq Spectra 26(3):601–617. https://doi.org/10.1193/1.3459159

Augenti N, Parisi F (2010) Learning from construction failures due to the 2009 L'Aquila, Italy, Earthquake. J Perform Constr Facil 24(6):536–555. https://doi.org/10.1061/(ASCE)CF.1943-5509.0000122

Bommer JJ, Acevedo AB (2004) The use of real earthquake accelerograms as input to dynamic analysis. J Earthq Eng 8:43–91. https://doi.org/10.1080/13632460409350521

Bommer JJ, Magenes G, Hancock J, Penazzo P (2004) The influence of strong-motion duration on the seismic response of masonry structures. Bull Earthq Eng 2:1–26. https://doi.org/10.1023/B:BEEE.0000038948.95616.bf

Calvi GM, Pinho R, Magenes G, Bommer JJ, Restrepo-Velez LF, Crowley H (2006) Development of seismic vulnerability assessment methodolgies or the past 30 years. ISET J Earthq Technol 43(3):75–104

Celik O C, Sesigur H (2010) Performance of Historic Masonry Buildings during the April 6, 2009 L'Aquila Earthquake. Paper presented at 14th European Conference on earthquake Engineering, Ohrid, Republic of North Macedonia, 30.08–03.09

Chaudhuri SR, Hutchinson TC (2004) Distribution of peak horizontal floor acceleration for estimating nonstructural element vulnerability. Conference paper presented at 13th World Conference on Earthquake Engineering, Vancouver, Canada, Paper No. 1721, 1–6th August

Chopra AK (2019) Dynamics of structures: theory and applications to earthquake engineering, 5th edn. Pearson, London

Cruz C, Miranda E (2016) Evaluation of damping ratios for the seismic analysis of tall buildings. J Struct Eng 143(1):1–10. https://doi.org/10.1061/(ASCE)ST.1943-541X.0001628

Cruz C, Miranda E (2017) A critical review of the Rayleigh damping model. Conference paper presented at 16th World Conference on Earthquake, Santiago, Chile

D'Amato M, Laguardia R, Trocchio GD, Coltellacci M, Gigliotti R (2020) Seismic risk assessment for masonry buildings typologies from L'Aquila 2009 earthquake damage data. J Earthq Eng. https://doi.org/10.1080/13632469.2020.1835750

D'Ayala D, Speranza E (2002) An integrated procedure for the assessment of seismic vulnerability of historic buildings. Conference paper at 12th European Conference on Earthquake Engineering, 561, London, UK

D'Ayala D (2013) Assessing the seismic vulnerability of masonry buildings. Handbook of Seismic Risk Analysis and Management of Civil Infrastructure Systems, Woodhead Publishing Series in Civil and Structural Engineering, pp 334–365. https://doi.org/10.1533/9780857098986.3.334

Drimmel J, Duma G (1974) Mitteilungen der Erdbeben-Kommission – Nr. 74 [Notices of the Earthquake Commission - No. 74]. Springer-Verlag, Vienna, Austria (in German)

Duma G (1988) Seismische Mikrozonierung des Stadtgebietes von Wien [Seismic microzonation of the urban area of Vienna]. Final report of the Federal Ministry of Science and Research and the City of Vienna, Vienna, Austria (in German)

Dunjic V (2018) Tragfähigkeitsbewertung ausgewählter gründerzeitlicher Mauerwerkskonstruktionen [Load carrying capacity analysis of select late 19th century masonry constructions]. Dissertation, Vienna University of Technology (in German)

Dynardo (2018) Elastoplastic material models for ANSYS general multisurface plasticity - multiPlas. Internal document. Dynardo GmbH, Weimar, Germany

FEMA P-154 (2015) Rapid visual screening of buildings for potential seismic hazards: A Handbook. 3rd ed. Applied Technology Council for the Federal Emergency Management Agency, FEMA, Washington, DC

Furtmüller T, Adam C (2011) Numerical modeling of the in-plane behavior of historical brick masonry walls. Acta Mech 221(1–2):65–77. https://doi.org/10.1007/s00707-011-0493-z

Furtmüller T, Adam C and Niederegger C (2012) Seismic capacity of old masonry buildings in Vienna: Numerical modeling of load-bearing brick masonry walls. Life-Cycle and Sustainability of Civil Infrastructure Systems: Proceedings of the 3rd International Symposium on Life-Cycle Civil Engineering (IALCCE 2012). Vienna, Austria. CRC Press, London. https://doi.org/10.1201/b12995

Ganz HR (1985) Mauerwerksscheiben unter Normalkraft und Schub [Masonry disks under normal force and shear]. Dissertation, ETH Zürich (in German)

Greguric M. (Forthcoming) Evaluierung der Erdbebensicherheit des Zagreber-Hochbaubestands nach dem Erdbeben vom 22. März 2020 [Evaluation of the seismic safety of the Zagreb building stock after the earthquake of March 22, 2020]. Master thesis, Vienna University of Technology (in German)

Grunthal G, Musson R M W, Schwartz J, Stucky M (1998) European macroseismic scale 1998 (EMS-98). European Seismological Commission: Working Group Macroseismic Scales, Luxembourg

Gutdeutsch R., Hammerl C, Mayer I, Vocelka K (1987) Erdbeben als historisches Ereignis. Die Rekonstruktion des Bebens von 1590 in Niederösterreich. [Earthquake as a historical event. The Reconstruction of the 1590 earthquake in Lower Austria]. Springer Verlag, Berlin Heidelberg (in German)

Hammerl C, Lenhardt WA (2013) Erdbeben in Niederösterreich von 1000 bis 2009 n. Chr. [Earthquakes in Lower Austria from 1000 to 2009 AD]. Treatises of the Federal Geological Survey, Vol. 67. Geological Survey of Austria (GBA), Vienna (in German)

Hancock J, Watson-Lamprey J, Abrahamson NA, Bommer JJ, Markatis A, McCoyh E, Mendis R (2006) An improved method of matching response spectra of recorded earthquake ground motion using wavelets. J Earthq Eng 10:67–89. https://doi.org/10.1080/13632460609350629

HCPI database (2020) GISbased building usability database. Croatian Center for Earthquake Engineering, Faculty of Civil Engineering, University of Zagreb and the Zagreb City, June (in Croatian). Accessed 20 Jan

Herak M, Allegretti I, Herak D, Ivancic I, Kuk V, Maric K, Markusic S, Sovic I (2011) Karta potresnih podrucja Hrvatske [Map of seismic areas in Croatia]. http://seizkarta.gfz.hr. Accessed 20 March 2021

Iervolino I, Cornell CA (2005) Record selection for nonlinear seismic analysis of structures. Earthq Spectra 21(3):685–713. https://doi.org/10.1193/1.1990199

Jordan J (2011) Effiziente Simulation großer Mauerwerksstrukturen mit diskreten Rissmodellen []. Dissertation, Technische Universität München (in German)

Karic A, Kolbitsch A (2020) Gründerzeitliche Mauerwerksbauten unter Erdbebeneinwirkung – Tragverhalten im Widerspruch zur aktuell angewandten Nachbemessung [HIstoric brick masonry buildings under earthquake action - load-bearing behavior in contradiction to currently applied post-design]. Mauerwerk 24(3):137–147: https://doi.org/10.1002/dama.202000009 (in German)

Karic A, Rudisch A, Kolbitsch A (2019) Verhalten von historischen Mauerwerksbauten unter Erdbebenbeanspruchung - Einfluss schubstarrer Decken auf die Erdbebensicherheit [Behavior of historic brick masonry buildings under seismic loading - influence of shear rigid slabs on seismic safety]. Bauingenieur 10: 2–9. https://doi.org/10.37544/0005-6650-2019-10-15 (in German)

Kita A, Cavalagli N, Masciotta MG, Lourenço PB, Ubertini F (2020) Rapid post-earthquake damage localization and quantification in masonry structures through multidimensional non-linear seismic IDA. Eng Struct 219:110841. https://doi.org/10.1016/j.engstruct.2020.110841

Kolbitsch A (1989) Altbaukonstruktionenen: Charakteristika Rechenwerte Sanierungsansätze [Old building structures: Characteristics computational values remediation approaches] Springer Verlag, Vienna

Kolbitsch A (2012) Assessment and retrofitting of façade elements of 19th century buildings. Conference paper at 15th World Conference on Earthquake Engineering, Lisbon, Portugal

Kopf F, Adam C (2014) Baudynamische Untersuchungen an Wiener Gründerzeithäusern [Dynamic investigations on historic brick masonry buildings]. Österreichische Ingenieur- Und Architekten-Zeitschrift 159:131–140

Krakora A, Bauer P (2014) Berechnungsbeispiele anhand des Wiener Gründerzeit – Mustergebäudes [Calculation examples based on the Viennese "Gründerzeit" - sample building]. Civil Engineering Division of Vienna/Lower Austria/ Burgenland, Vienna, Austria

Loli M, Anastasopoulos I, Gazetas G (2015) Nonlinear analysis of earthquake fault rupture interaction with historic masonry buildings. Bull Earthq Eng 13:83–95. https://doi.org/10.1007/s10518-014-9607-z

Lu S, Heuer R (2007) Seismic assessment of lifeline masonry structures using an advanced material model. Struct Control Health Monit 14:321–332

Meinhardt C (2008) Einflussgrößen für das Schwingungsverhalten von Gebäuden zur Prognose von Erschütterungsimmissionen [Influencing variables for the dynamic behavior of buildings for the prediction of vibration immissions]. Dissertation. Berlin University of Technology (in German)

Meskouris KH, Sadegh-Azar H, Berezowsky H, Dümling R (2001) Schnellbewertung der Erdbebengefährung von Gebäuden [Rapid assessment of the seismic hazard of buildings]. Bauingenieur 7(8):370–376 **(in German)**

Meskouris KH, Hinzen KG, Butenweg C, Mistler M (2011) Bauwerke und Erdbeben: Grundlagen – Anwendung – Beispiele [Structures and earthquakes: Fundamentals - Application - Examples]. Vieweg + Teubner Verlag, Wiesbaden (in German)

Moschen L, Tsalouchidis K T, Adam C (2019) Tragwerksantwort Wiener Gründerzeithäuser unter Erdbebenanregung auf Grundlage des Wiener Erdbebensatzes [Seismic response of Viennese brick masonry buildings based on the Viennese ground motion set]. Bauingenieur 12:461–471. https://doi.org/10.37544/0005-6650-2019-12-23

ÖN EN 1998–1 (2013) Eurocode 8: Auslegung von Bauwerken gegen Erdbeben - Teil 1: Grundlagen, Erdbebeneinwirkungen und Regeln für Hochbauten [Eurocode 8: Design of structures for earthquake resistance - Part 1: General rules, seismic actions and rules for buildings]. Austrian Standards Institute, Austria

ÖN B 1998–1 (2017) Eurocode 8: Eurocode 8: Auslegung von Bauwerken gegen Erdbeben - Teil 1: Grundlagen, Erdbebeneinwirkungen und Regeln für Hochbauten - Nationale Festlegungen zu ÖNORM EN 1998–1 und nationale Erläuterungen [Eurocode 8: Design of structures for earthquake resistance - Part

1: General rules, seismic actions and rules for buildings - National specifications concerning ÖNORM EN 1998–1 and national comments]. Austrian Standards Institute, Austria
ÖN EN 1998–3 (2013) Eurocode 8: Auslegung von Bauwerken gegen Erdbeben – Teil 3: Beurteilung und Ertüchtigung von Gebäuden [Eurocode 8: Design of structures for earthquake resistance - Part 3: Assessment and retrofitting of buildings]. Austrian Standards Institute, Austria
PEER (2010) Pacific earthquake engineering research center: PEER ground motion database. University of California, Berkeley, p 2010
Rayleigh JWSB, Lindsay RB (1945) The Theory of Sound: Volume 1. 2nd edn. Dover Publications Inc, New York
Rossetto T, Peiris N, Alarcon JE, So E, Sargeant S, Free M, Sword-Daniels V, Del Re D, Libberton C, Verrucci E et al (2011) Field observations from the Aquila, Italy earthquake of April 6, 2009. Bull Earthq Eng 9:11–37. https://doi.org/10.1007/s10518-010-9221-7
Rota M, Penna A, Strobbia CL (2008) Processing Italian damage data to derive typological fragility curves. Soil Dyn Earthq Eng 28:933–947. https://doi.org/10.1016/j.soildyn.2007.10.010
Rudisch A, Dunjic V, Kolbitsch A (2017) Investigation of horizontal floor acceleration in historic masonry buildings. Mauerwerk 21(6):348–356. https://doi.org/10.1002/dama.201700017
Savor Novak M, Uros M, Atalic J, Herak M, Demsic M, Banicek M, Lazarevic D, Bijelic N, Crnogorac M, Todoric M (2020) Zagreb earthquake of 22 March 2020 – preliminary report on seismologic aspects and damage to buildings. J Croatian Assoc Civil Eng 72(10):843–867
Schubert P (2010) Eigenschaftswerte von Mauerwerk, Mauersteinen, Mauermörtel und Putzen [Property values of masonry, masonry units, masonry mortar and plasters]. Mauerwerk-Kalender 2010:3–25. Ernst & Sohn, Berlin. (in German)
Schlegel R (2004) Numerische Berechnung von Mauerwerkstrukturen in homogenen und diskreten Modellierungsstrategien [Numerical calculation of masonry structures in homogeneous and discrete modeling strategies]. Dissertation, Bauhaus-Universität Weimar (in German)
Schlegel R, Will J, Rautenstrauch K (2004) Materialmodelle für nichtlineare Berechnungen komplexer Mauerwerkstrukturen mit ANSYS [Material models for nonlinear analysis of complex masonry structures with ANSYS]. Conference paper at International Congress on FEM Technology with ANSYS CFX & ICEM CFD. Dresden, Germany
Schwarz J, Beinersdorf S, Langhammer T, Leipold M (2010) Verhalten von Mauerwerksbauten unter Erdbebeneinwirkung: Auswertung der Schäden des Albstadt-Erdbebens vom 3.[Vulnerability of masonry structures under seismic action: Damage analysis of the September 3, 1978 Albstadt earthquake. Mauerwerk 14(3):126–135. https://doi.org/10.1002/dama.201000467
SeismoMatch (Version 2020) (2020) Earthquake Software for Response Spectrum Matching. Seismosoft, Pavia, Italy
Simović V (2000) Potresi na zagrebačkom području [Earthquakes in Zagreb area]. J Croatian Assoc Civil Eng 52(11):637–645
SIA 269/8 (2017) Erhaltung von Tragwerken – Erdbeben [Structural preservation - Earthquake]. Schweizerischer Ingenieur- und Architektenverein (SIA), Zürich, Switzerland
Simo JC, Hughes TJR (1998) Computational inelasticity. Springer, New York. https://doi.org/10.1007/b98904
Song Z, Su C (2017) Computation of rayleigh damping coefficients for the seismic analysis of a hydropowerhouse. shock and vibration, 2046345:11. https://doi.org/10.1155/2017/2046345
Tomazevic M (1999) Earthquake-resistant design of masonry buildings. Imperial College Press, London
Uros M, Savor Novak M, Atalic J, Sigmund Z, Banicek M, Demsic M, Hak S (2020) Procjena oštećenja građevina nakon potresa - postupak provođenja pregleda zgrada [Post-earthquake damage assessment of buildings – procedure for conducting building inspections]. Journal of the Croatian Association of Civil Engineers 72, 12: 1089–1115. https://doi.org/10.14256/JCE.2969.2020 (in Croatian)
Zimmermann T, Strauss A (2012) Schubtragfähigkeit von altem unbewehrtem Mauerwerk unter seismischer Belastung [Shear capacity of old unreinforced masonry under seismic loading]. Bautechnik 89(8):553–563. https://doi.org/10.1002/bate.201201564

Terms and Conditions

Springer Nature journal content, brought to you courtesy of Springer Nature Customer Service Center GmbH ("Springer Nature").

Springer Nature supports a reasonable amount of sharing of research papers by authors, subscribers and authorised users ("Users"), for small-scale personal, non-commercial use provided that all copyright, trade and service marks and other proprietary notices are maintained. By accessing, sharing, receiving or otherwise using the Springer Nature journal content you agree to these terms of use ("Terms"). For these purposes, Springer Nature considers academic use (by researchers and students) to be non-commercial.

These Terms are supplementary and will apply in addition to any applicable website terms and conditions, a relevant site licence or a personal subscription. These Terms will prevail over any conflict or ambiguity with regards to the relevant terms, a site licence or a personal subscription (to the extent of the conflict or ambiguity only). For Creative Commons-licensed articles, the terms of the Creative Commons license used will apply.

We collect and use personal data to provide access to the Springer Nature journal content. We may also use these personal data internally within ResearchGate and Springer Nature and as agreed share it, in an anonymised way, for purposes of tracking, analysis and reporting. We will not otherwise disclose your personal data outside the ResearchGate or the Springer Nature group of companies unless we have your permission as detailed in the Privacy Policy.

While Users may use the Springer Nature journal content for small scale, personal non-commercial use, it is important to note that Users may not:

1. use such content for the purpose of providing other users with access on a regular or large scale basis or as a means to circumvent access control;
2. use such content where to do so would be considered a criminal or statutory offence in any jurisdiction, or gives rise to civil liability, or is otherwise unlawful;
3. falsely or misleadingly imply or suggest endorsement, approval , sponsorship, or association unless explicitly agreed to by Springer Nature in writing;
4. use bots or other automated methods to access the content or redirect messages
5. override any security feature or exclusionary protocol; or
6. share the content in order to create substitute for Springer Nature products or services or a systematic database of Springer Nature journal content.

In line with the restriction against commercial use, Springer Nature does not permit the creation of a product or service that creates revenue, royalties, rent or income from our content or its inclusion as part of a paid for service or for other commercial gain. Springer Nature journal content cannot be used for inter-library loans and librarians may not upload Springer Nature journal content on a large scale into their, or any other, institutional repository.

These terms of use are reviewed regularly and may be amended at any time. Springer Nature is not obligated to publish any information or content on this website and may remove it or features or functionality at our sole discretion, at any time with or without notice. Springer Nature may revoke this licence to you at any time and remove access to any copies of the Springer Nature journal content which have been saved.

To the fullest extent permitted by law, Springer Nature makes no warranties, representations or guarantees to Users, either express or implied with respect to the Springer nature journal content and all parties disclaim and waive any implied warranties or warranties imposed by law, including merchantability or fitness for any particular purpose.

Please note that these rights do not automatically extend to content, data or other material published by Springer Nature that may be licensed from third parties.

If you would like to use or distribute our Springer Nature journal content to a wider audience or on a regular basis or in any other manner not expressly permitted by these Terms, please contact Springer Nature at

onlineservice@springernature.com